AIAA 2013-4220

JBLADE: a Propeller Design and Analysis Code

Silvestre, M. A. R.[1] Morgado, J.[2] and Páscoa, J. C.[3]
University of Beira Interior, Covilhã, 6200-001, Portugal

This paper presents the methodology and numerical implementation of a propeller analysis tool. The code has the capability to estimate the performance curves of a given design for use in off-design evaluation. The long term goal of the JBLADE development is to provide a user-friendly, accurate, and validated open-source code that can be used to design and optimize a variety of propellers. The code allows the introduction of the blade geometry as an arbitrary number of sections characterized by their radial position, chord, twist, length and airfoil coordinates. The propeller number of blades and hub radius must be specified as well. The code was used to compute the performance of the propeller data from NACA Technical Report No. 594 and the results were checked against QPROP and JAVAPROP numerical codes as well as against to the experimental data.

Downloaded by UNIV OF TEXAS AUSTIN on August 16, 2013 | http://arc.aiaa.org | DOI: 10.2514/6.2013-4220

Nomenclature

C_L	=	*Airfoil lift coefficient*
C_D	=	*Airfoil drag coefficient*
D	=	*Propeller diameter*
F	=	*Prandtl's factor*
C_a	=	*Normal force coefficient*
C_t	=	*Tangential force coefficient*
c	=	*Blade local chord*
B	=	*Number of blades*
r	=	*Radius of blade element position*
a_a	=	*Axial induction factor*
a_t	=	*Tangential induction factor*
L	=	*Lift Force*
W	=	*Element relative velocity*
T	=	*Thrust*
Q	=	*Torque*
P	=	Power
n	=	*Rotation speed*
t	=	*Airfoil thickness*
c_t	=	*Thrust coefficient*
c_p	=	*Power coefficient*
ρ	=	*Air density*
α	=	*Angle of attack*
ϕ	=	*Inflow angle*
θ	=	*Incidence angle*
σ	=	*Local rotor solidity ratio*

[1] Assistant Professor, Aerospace Sciences Department, Rua Marquês D'Ávila e Bolama, Senior Member of AIAA, corresponding author.
[2] PhD Student, Aerospace Sciences Department, Rua Marquês D'Ávila e Bolama, Student Member of AIAA.
[3] Assistant Professor, Electromechanics Department, Rua Marquês D'Ávila e Bolama.

Copyright © 2013 by Miguel Angelo Rodrigues Silvestre. Published by the American Institute of Aeronautics and Astronautics, Inc., with permission.

I. Introduction

THE problems caused by growth in the transportation sector, *e.g.* the rise of fuel consumption and cost, as well as pollution and consequent climate change led to a reconsideration of the transportation systems by the most economically advanced nations[1]. Nowadays, despite all technologic developments, as we proceed in the 21st century, we may be about to witness the return of slower transportation as a mean of increasing energy efficiency and business profitability. Regarding air transportation, open rotors propulsion systems are being considered for future airliners[2] in the past, unducted fans have been developed that delivered better specific fuel consumption (SFC) than the ultra high bypass ratio turbofans being developed today. In both cases, the noise is an issue. Reducing the tip speed of these devices is an obvious solution for noise but requires a reduction of cruise speed and disk loading and the side effects are further reductions in drag and SFC. All of this means that we may well witness the return of propellers for future commercial aviation.

Slowing down aircrafts can take us towards the airship. After the initial developments until the 30s, and during some decades, the airships were only considered as a mere curiosity. At their peak, in the late 30s, airships were unrivaled in transoceanic transportation. Nowadays, they can be used effectively as platforms for different purposes[3–6] specially activities that requires long endurance and requires hovering for long times. In Europe, the development of the new airships is also being supported by European Union through the Multibody Concept for Advanced Airship for Transport (MAAT[7]) project. This collaborative project involves 12 different institutions and aims to develop a heavy lift cruiser-feeder airship system in order to provide middle and long range transport for passengers and goods. Since MAAT project has the objective of operating an airship at stratospheric altitudes, propellers are a valid option to the airship propulsion[8]. In this particular project, as well as in other cases of rotary or fixed wing crafts for vertical and short take off and landing, the maximization of static thrust per unit shaft power is an important goal. Thus, it is crucial to have a numerical tool suitable for the optimization of propellers. An airship propeller must be efficient in thrust per unit power for the hovering flight condition as well as it must have a high propulsive efficiency for cruise flight. For this multipoint optimization of the propeller design and off-design performance analysis, CFD tends to be time consuming and expensive. The most common way to do optimization is based in the analysis of numerous designs as to compare their relative merits. This can be only achieved with low computational cost numerical tools. The use of low order codes in the early stages of design enables higher fidelity CFD calculations or wind tunnel tests to be performed on more mature designs.

The first developments related to the theory of propellers occurred in 19th century with Rankine and Froude[9] through a work focused on marine propellers. They presented the primary momentum relations governing a propulsive mechanism in a water medium. Later, Drzewiecki[10] presented the blade element theory. In this theory each element of the blade can be treated as an individual lifting surface moving through the air on a helical path. However, he did not take into account the effect of the propeller induced velocity on each element. In 1919, Betz[11] stated that the load distribution for lightly loaded propellers with minimum energy loss is such that the shed vorticity forms regular helicoidal vortex sheets moving backward undeformed behind the propeller. Thus, the induced losses of propellers will be minimized if the propeller slipstream has a constant axial velocity and if each cross section of the slipstream rotates around the propeller axis like a rigid disk[12]. However, the ideal case described by Betz cannot be achieved with a propeller with a finite number of blades.

Prandtl[10] found an approximation to the flow around helicoidal vortex sheets which is good if the advance ratio is small and improves as the number of blades increases[13]. The approximation presented by Prandtl is still applied in simple mathematical codes. Later, Goldstein[14] found a solution for the potential field and the distribution of circulation for propellers with small advance ratios. He has shown that the vortex sheets shed from the trailing edges of propeller blades cannot move as rigid bodies. In addition, he has presented the values for the circulation's distribution for lightly loaded propellers with two and four blades. Theodorsen[15], through his study on the vortex system in the far field of the propeller, concluded that the Goldstein's solution for the field of a helicoidal vortex sheet remains valid, even for moderate/highly loaded propellers. He also elaborated the theory of propellers with an ideal load distribution, based on the analysis of helicoidal trailing vortex sheets and the thrust and torque implied by their form and displacement velocity. In 1980, Larrabee[16] analyzed the steady airloads on the propeller and presented a practical design theory for minimum induced loss propellers. This method is a combination between momentum theory, blade element theory and vortex theory. Later on, Adkins[17] presented improvements with small angle approximations and light load approximations, overcoming the restrictions in the method developed by Larrabee.

JBLADE is a numerical open-source propeller design and analysis code written in the Qt® programming language. The code is based on David Marten's QBLADE[18,19] and André Deperrois's XFLR5[20] codes. It uses the classical Blade Element Momentum (BEM) theory modified to account for three dimensional flow equilibrium. Its

Downloaded by UNIV OF TEXAS AUSTIN on August 16, 2013 | http://arc.aiaa.org | DOI: 10.2514/6.2013-4220

Copyright © 2013 by Miguel Angelo Rodrigues Silvestre. Published by the American Institute of Aeronautics and Astronautics, Inc., with permission.

methodology and theoretical formulation for propeller analysis are presented herein. The code can estimate the performance curves of a given design for off-design analysis. The software has a graphical interface making easier to build and analise the propeller simulations. The long term goal of the JBLADE is to provide a user-friendly, accurate, and validated open-source code that can be used to design and optimize a variety of propellers.

The airfoil performance figures needed for the blades simulation come from QBLADE's coupling with the open-source code XFOIL[21]. This integration, which is also being improved, allows the fast design of custom airfoils and computation of their lift and drag polars. In addition, it is possible to integrate extrapolated or wind tunnel airfoil data polars in the propeller simulation.

II. Code Structure

The JBLADE code allows the introduction of the blade geometry as an arbitrary number of sections characterized by their radial position, chord, twist, length, airfoil and associated complete angle of attack range airfoil polar. The code provides a 3D graphical view of blade to the user (see Figure 1), helping the user to detect inconsistencies. The propeller number of blades and hub radius must be specified as well. JBLADE allows a direct visualization of simulation results through a graphical user interface making the software accessible and easy to understand by willing users. In addition, the coupling between different JBLADE modules avoid time consuming operations of importing/exporting data, decreasing possible mistakes created by the user.

An overview of the code structure with the different data objects submodules and iteration routines in which the polars, blades, propellers and simulations defined, executed are stored is shown in Figure 2. In addition, it can be seen how the BEM module is coupled with XFOIL module.

The simulation starts being built by importing the blade's sections airfoils coordinates into the XFOIL module. A direct analysis for each airfoil performance over the largest possible angle of attack range is performed. It is important that the actual blade operation Reynolds and Mach number are defined in the XFOIL simulations. So, some iteration may be needed for a complete propeller simulation. These XFOIL airfoils performance polars are used in the 360º Polar Object, where a full 360º range of angle of attack airfoil polar for each blade section airfoil is built. Each 360º polar is defined by its name and parent XFOIL polar.

After at least one 360º Polar is stored in the 360º Polar Object database sub-module, a blade can be defined in the Blade object sub-module. This sub-module stores the blades' geometric data as well as which 360º polar is associated to each of the blade sections previously defined in Blade Object. The propeller data is stored in the Propeller Object sub-module. The Propeller Simulation Object sub-module is used when a simulation is defined to store the simulation parameters. The simulation results, which characterize the propeller performance are obtained in BEM simulation routine sub-module and stored in the Blade Data Object sub-module for each element along the blade and added to the Propeller Simulation Object database.

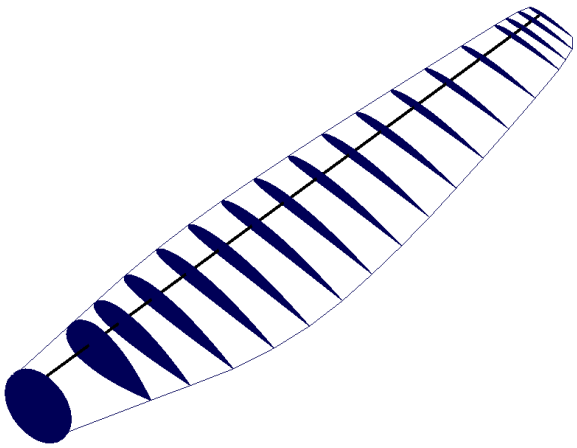

Figure 1. Example of blade visualization in JBLADE.

Downloaded by UNIV OF TEXAS AUSTIN on August 16, 2013 | http://arc.aiaa.org | DOI: 10.2514/6.2013-4220

Copyright © 2013 by Miguel Angelo Rodrigues Silvestre. Published by the American Institute of Aeronautics and Astronautics, Inc., with permission.

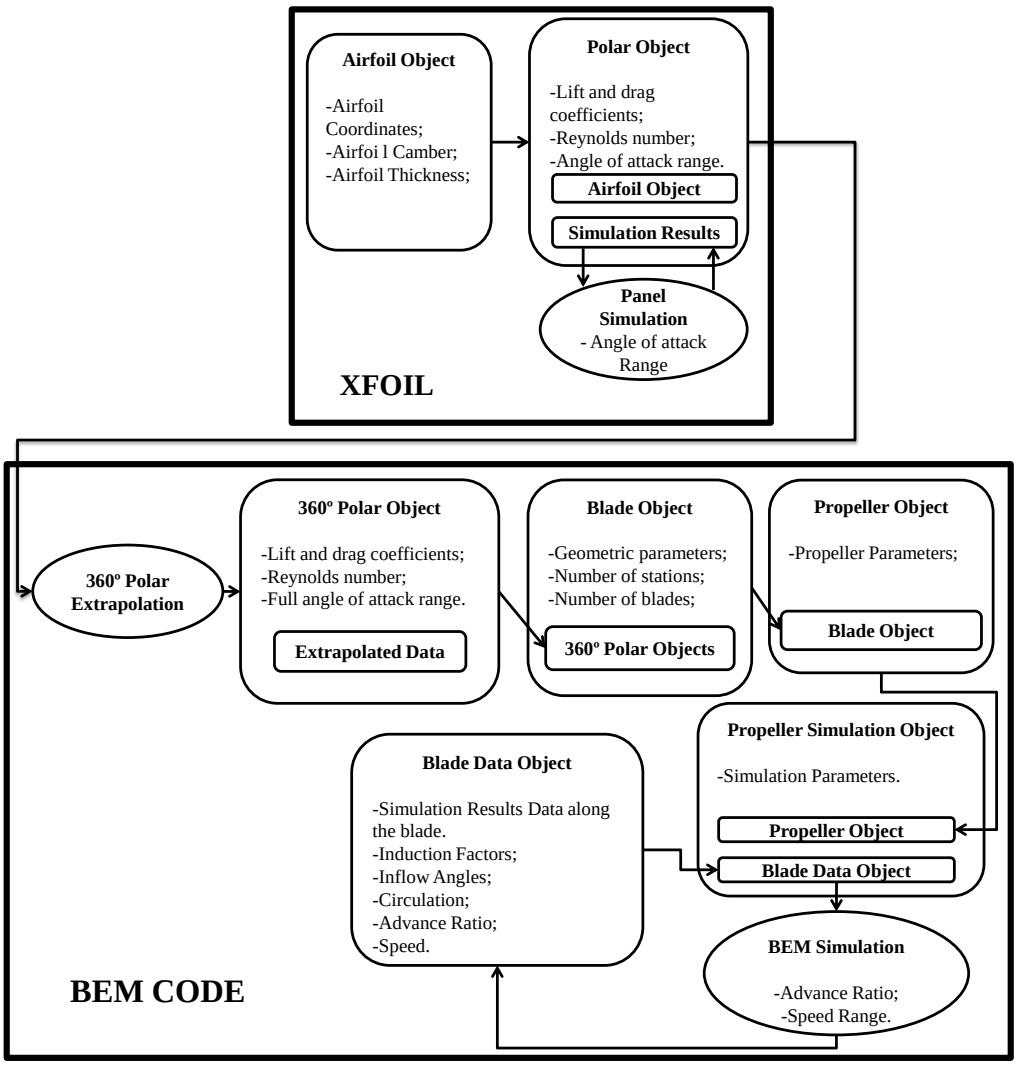

Figure 2. JBLADE code structure.

III. Theoretical Formulation

A. Classical Blade Element Momentum Theory

The propeller blade is divided into a set of blade elements. Each blade element is a discrete rotating wing (see Figure 3). The blade element relative windspeed, W, and respective inflow angle, ϕ, are computed through the axial and tangential velocity components, W_a and W_t, respectively. W_a results from the sum of the propeller airspeed, V to the induced axial velocity, V_a, at the propeller disk, W_t results from the sum of the velocity of the element due to the propeller rotation, Ωr, with the induced tangential velocity, V_t. The induced velocity components are determined from the momentum theory, for the annulus sweeped by the rotating blade element and used to calculate the angle of attack, α, as the difference between ϕ and local incidence angle, θ, With α, the element's lift and drag coefficients, C_L and C_D can be determined. With these coefficients, the axial and tangential force coefficients, C_a, C_t are obtained according to the local θ:

$$C_a = C_L \cos\phi - C_D \sin\phi \tag{1}$$

$$C_t = C_L \sin\phi + C_D \cos\phi \tag{2}$$

Downloaded by UNIV OF TEXAS AUSTIN on August 16, 2013 | http://arc.aiaa.org | DOI: 10.2514/6.2013-4220

Copyright © 2013 by Miguel Angelo Rodrigues Silvestre. Published by the American Institute of Aeronautics and Astronautics, Inc., with permission.

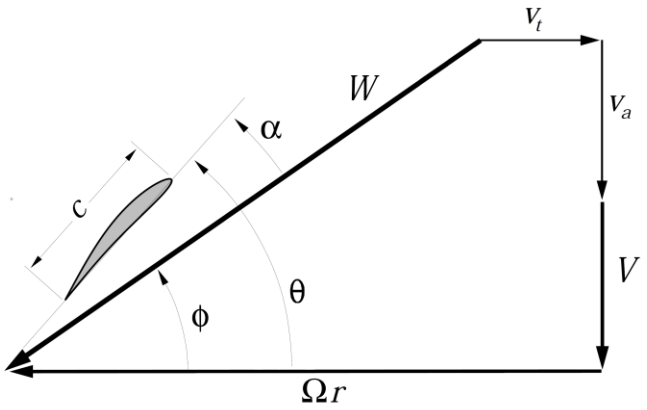

Figure 3. Blade geometry and velocity triangle at an arbitrary radius blade position.[22]

To describe the overall propeller performance, the forces are obtained from the force coefficients according to:

$$F_x = \frac{1}{2}\rho W^2 c C_x \tag{3}$$

The total thrust and torque of the propeller are calculated from

$$T = B\int_{R_{root}}^{R_{tip}} F_a dr \tag{4}$$

$$Q = B\int_{R_{root}}^{R_{tip}} F_t r dr \tag{5}$$

With the total torque from Eq. (5), the necessary shaft power is obtained,

$$P = \Omega Q \tag{6}$$

and dimensionless thrust and power coefficients are calculated from their definitions:

$$c_t = \frac{T}{\rho n^2 D^4} \tag{7}$$

$$c_p = \frac{P}{\rho n^3 D^5} \tag{8}$$

When the advance ratio is defined as presented in Eq.(9), the propeller efficiency is computed through Eq. **(10)**:

$$J = \frac{v}{nD} \tag{9}$$

$$\eta = \frac{c_t}{c_p} J \tag{10}$$

Downloaded by UNIV OF TEXAS AUSTIN on August 16, 2013 | http://arc.aiaa.org | DOI: 10.2514/6.2013-4220

Copyright © 2013 by Miguel Angelo Rodrigues Silvestre. Published by the American Institute of Aeronautics and Astronautics, Inc., with permission.

The iteration variables of the classical BEM method are the axial and tangential induction factors, defined from the induced velocity components as:

$$a_a = \frac{W_a - V}{V} \tag{11}$$

$$a_t = \frac{W_t - \Omega r}{\Omega r} \tag{12}$$

and derived from momentum theory:

$$a_a = \left(\frac{4F \sin^2 \phi}{\sigma c_a} - 1 \right)^{-1} \tag{13}$$

$$a_t = \left(\frac{4F \sin\phi \cos\phi}{\sigma c_t} + 1 \right)^{-1} \tag{14}$$

Where σ is the local rotor solidity ratio, which is the ratio of the blade element area to the annulus sweep by the element in its rotation, and it is defined by Eq. (15):

$$\sigma = \frac{cB}{2\pi r} \tag{15}$$

and F is the Prandtl's correction factor. It compensates for the amount of work that can actually be performed by the element according to its proximity to the blade's root or tip. If the element is at the blade tip, its contribution will be zero (F=0). F is estimated according to Eq. (16) in the 3D corrections model.

To compute the inflow angle ϕ, the induction factors must be known. An arbitrary value is assigned for both axial and tangential induction factors for the first iteration. The iteration is repeated for all blade elements.

Thus, with lift and drag coefficients for the angle of attack, the induction factors are updated and compared to the ones from the previous iteration. As soon as the difference is below the convergence criteria defined by the user, the iteration stops and the next blade element is computed.

B. 3D Corrections

During each iteration, the code also takes into account the losses caused by tip and root vortices. These corrections, originally implemented by Prandtl[13], are modeled by:

$$F = \frac{2}{\pi} a\cos\left(e^{-f}\right) \tag{16}$$

where:

$$f_{root} = \frac{B}{2}\left(1 + \frac{R_{root}}{r}\right)\frac{1}{g} \tag{17}$$

$$g_{root} = \frac{R_{root}}{r}\tan\phi \tag{18}$$

or:

$$f_{tip} = \frac{B}{2}\left(1 - \frac{r}{R_{tip}}\right)\frac{1}{g} \tag{19}$$

$$g_{tip} = \frac{r}{R_{tip}}\tan\phi \tag{20}$$

Downloaded by UNIV OF TEXAS AUSTIN on August 16, 2013 | http://arc.aiaa.org | DOI: 10.2514/6.2013-4220

Copyright © 2013 by Miguel Angelo Rodrigues Silvestre. Published by the American Institute of Aeronautics and Astronautics, Inc., with permission.

C. 3D Equilibrium

The theoretical formulation presented above assumes that the flow in the propeller annulus is two dimensional, meaning neglects radial movement of the flow is ignored. But for such condition, tridimensional equilibrium[23] must exist. This can be modeled from Eq. (21):

$$W_a \frac{\partial W_a}{\partial r} + W_t \frac{\partial W_t}{\partial r} + \frac{W_t^2}{r} = 0 \tag{21}$$

The case where W_a is maintained constant across the propeller annulus, reduces Eq. (21) to:

$$\frac{dW_t}{dr} = -\frac{W_t}{r} \Leftrightarrow W_t r = const. \tag{22}$$

In this case, the whirl varies inversely with radius, which is best known as the free vortex condition. Although this differs substantially from the ordinary BEM approach where the momentum theory applied to the tangential velocity induction totally disregards the neighbor elements to determine the element's V_t, it makes sense when one considers that from far upstream down to the propeller disk, the flow should be isentropic or close to irrotational, thus respecting the free vortex condition. To implement this equilibrium condition, in first iteration the forces coefficients are computed assuming no tangential induction factor, which means that $a_t = 0$. The element *i* annulus mass flow rate is calculated as,

$$\dot{m}_i = 2\rho W_a \pi r dr \tag{23}$$

and

$$\dot{m}_{total} = \sum \dot{m}_i \tag{24}$$

To satisfy the momentum conservation, the total propeller torque will be the result of a free vortex induced tangential velocity profile with an average axial velocity, $\overline{W_a}$ across the propeller disk. A reference value of tangential induced velocity is used that corresponds to that at 75% of the blade radius position, $V_{t_{75}}$. The average axial velocity is:

$$\overline{W_a} = \frac{\dot{m}_{total}}{\pi \rho R^2} \tag{25}$$

According to Eq.**(26)**, at a given element, V_t is:

$$V_t = \frac{0.75 R V_{t_{75}}}{r} \tag{26}$$

$$Q = \int 4\pi\rho \overline{W_a} V_t r dr \tag{27}$$

Thus, replacing Eq. (25) and (26) in Eq. (27) and solving for $V_{t_{75}}$

$$V_{t_{75}} = \frac{Q}{3\pi\rho \overline{W_a} R\left(R_{tip} - R_{root}\right)} \tag{28}$$

Downloaded by UNIV OF TEXAS AUSTIN on August 16, 2013 | http://arc.aiaa.org | DOI: 10.2514/6.2013-4220

Copyright © 2013 by Miguel Angelo Rodrigues Silvestre. Published by the American Institute of Aeronautics and Astronautics, Inc., with permission.

The radial induction factor can be updated and the coefficients will be calculated again with the updated radial induction factor.

$$a_t = \frac{V_t}{\Omega r} \tag{29}$$

D. Post Stall Model

The rotational motion of the blade affects the element's boundary layer such that the airfoil stall shifts to higher angles of attack. So, a correction for the mentioned problem is also present in JBLADE. The correction is based on the work of Corrigan and Schillings[24] and is presented in Eq. (30). This model is based on local solidity ratio and relates the stall delay to the ratio of the local blade chord to radial position.

$$c_{rot(\alpha+\Delta\alpha)} = c_{non-rot}\left(\frac{dc_l}{d\alpha}\Delta\alpha\right) \tag{30}$$

where:

$$\Delta\alpha = \left[\left(\frac{K\left(\frac{c}{r}\right)}{0.136}\right)^n - 1\right]\left(\alpha_{C_{L_{\max}}} - \alpha_{C_{L_0}}\right)$$

The separation point is related with the velocity gradient, K through Eq. (31):

$$\left(\frac{c}{r}\right) = 0.1517K^{-1.084} \tag{31}$$

IV. Results and Discussion

A. Test Case

In order to validate JBLADE code, a propeller described in NACA Technical Report No. 594[25] was simulated. This propeller has the Clark Y airfoil with variable thickness, *t*, along the blade span sections and 3 blades. Details of propeller geometry and data for different blade pitch angles can be seen in Figure 4. The investigated propeller corresponds to the configuration named "Nose 6 – Propeller C".

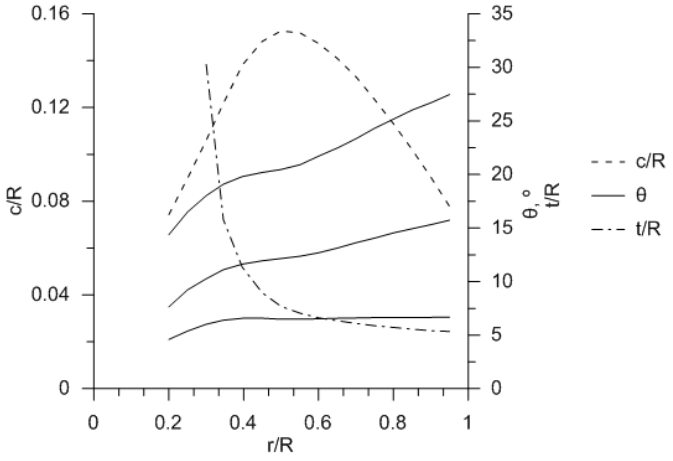

Figure 4. Propeller Geometry presented in NACA Technical Report No. 594[25]. Propeller has 3 blades and a diameter of 3.054 meters.

Downloaded by UNIV OF TEXAS AUSTIN on August 16, 2013 | http://arc.aiaa.org | DOI: 10.2514/6.2013-4220

Copyright © 2013 by Miguel Angelo Rodrigues Silvestre. Published by the American Institute of Aeronautics and Astronautics, Inc., with permission.

The airfoil polars were obtained with the code's XFOIL module, with a specified Reynolds and Mach numbers distribution. These polars were extrapolated such that the lift and drag coefficients became available for 360º airfoil angle of attack range. Geometry presented in the Figure 4 was replicated in JBLADE's Blade Object sub-module and the corresponding airfoil for each blade section was used. The blade pitch angle was adjusted to the given angle at 75% of the radius and the propeller performance was computed.

B. Propeller Simulation

To simulate the propeller in JBLADE, the number of needed points to define the airfoil coordinates in order to optimize XFOIL numerical accuracy was firstly studied. In Figure 5 are presented the different polars obtained with different number of points in the airfoil definition. It was concluded that for more than 200 points, XFOIL does not show a significant difference in the resulting airfoil polars, and that each airfoil should be redefined to that number of points.

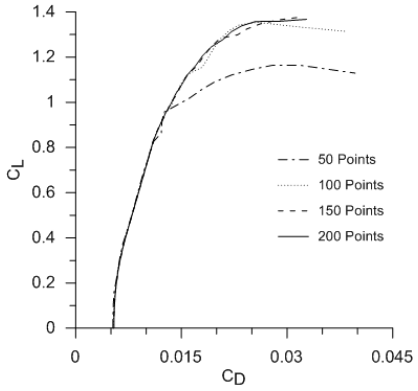

Figure 5. Validation of polars calculations using different number of points to define an airfoil in XFOIL.

To validate the computations for a wide range of advance ratios, independent simulations for small and big advance ratios were computed and compared with the previously calculated curve using an average distribution of Reynolds and Mach numbers along the blade (see Figure 6). For each of the blade section the average Reynolds and Mach number was set as the mean value corresponding to half the advance ratio that corresponded to the propeller operating conditions used to collect the experimental data.

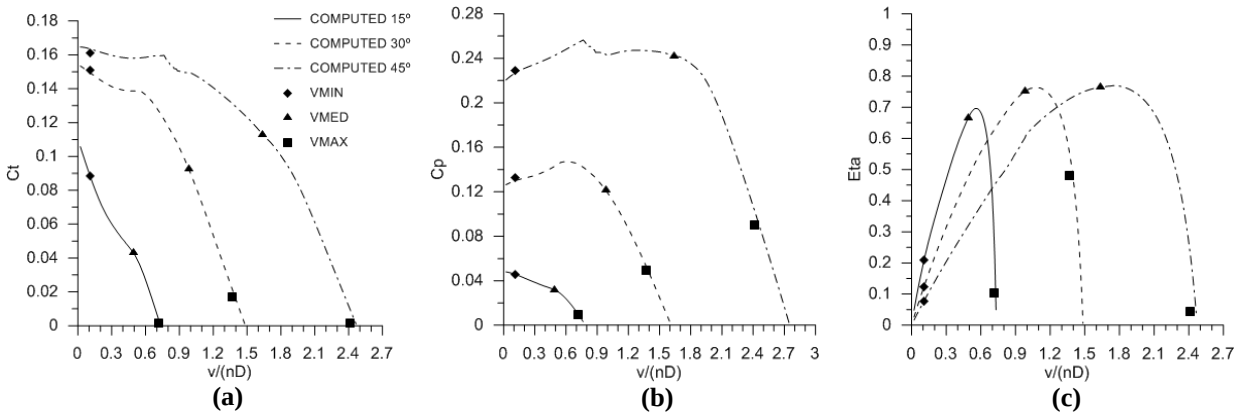

Figure 6. Validation of calculations using a distribution of averaged Reynolds and Mach Numbers along the blade: (a) – Thrust Coefficient (b) – Power Coefficient, (c) – Propeller Efficiency.

Downloaded by UNIV OF TEXAS AUSTIN on August 16, 2013 | http://arc.aiaa.org | DOI: 10.2514/6.2013-4220

Copyright © 2013 by Miguel Angelo Rodrigues Silvestre. Published by the American Institute of Aeronautics and Astronautics, Inc., with permission.

To obtain *VMIN* points, the distribution of Reynolds and Mach numbers were collected for a low airspeed operating condition. The propeller rotational speed is constant at 3,000 rpm. The airfoil polars were calculated using those Reynolds and Mach numbers and new airfoil polars were associated to a new propeller. The propeller performance was only analyzed for that specified speed. The *VMAX* points were obtained with same procedure but for an airspeed close to the zero thrust condition. The *COMPUTED* curves were calculated with the Reynolds and Mach numbers distributions collected for *VMED* points. VMED is the airspeed in the middle of VMIN and VMAX. These VMED averaged Reynolds and Mach numbers distribution allow a close approximation for the full range of advance ratios simplifiyng the simulation throughout.

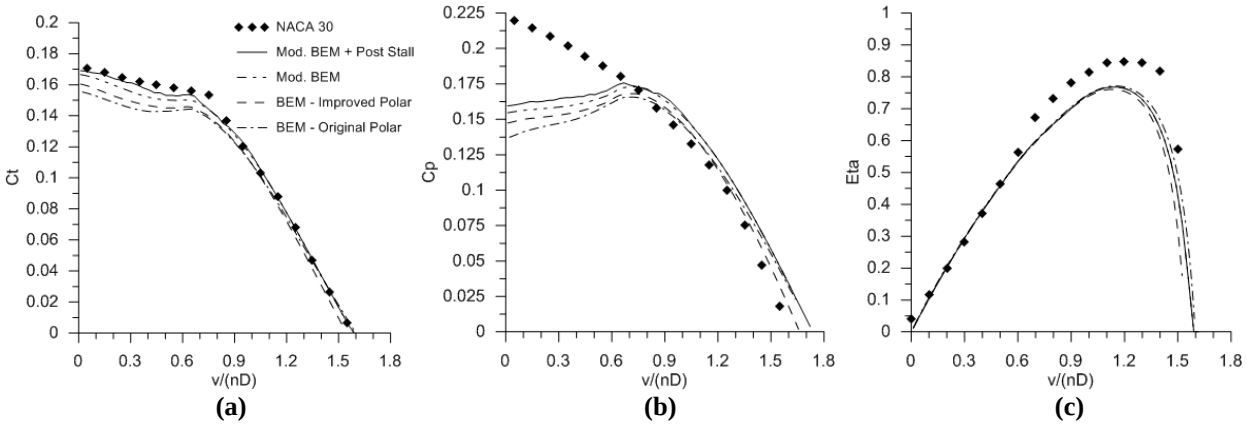

Figure 7. Modelation influence on the simulated propeller performance.

The history of the improvements on the theoretical formulation of JBLADE can be seen in Figure 7. "BEM + Original Polar" was the initial formulation as it was incorporated in QBLADE for wind turbines but extended here to simulate propellers. "BEM + Improved Polar" corresponds to the modified 360º range of angle of attack polars model improvement[26] with a visible improvement in the prediction of the thrust and power coefficients at low advance ratios and a slight under prediction at high advance ratios for the thrust coefficient. "Mod. BEM" corresponds to the modification of the classical BEM with the 3D equilibrium described in section III.C. resulting in significant improvements throughout the complete advance ratio range. "Mod. BEM + Post Stall" includes the post stall model described in section III.D. and corresponds to the final formulation used in the simulations thereafter.

C. Results

Figure 8 shows that JBLADE predicts closely the thrust coefficient; however, the power coefficient is significantly under predicted at low advance ratios and slightly over estimated in the higher end. It was found in the first case that the cause may be attributed to the airfoil's 360º angle of attack range airfoil polar misrepresentation just above the stall since that at the lower advance ratios together with high pitch angles; there is a significant portion of the blade root well into deep stall angles of attack. The propeller efficiency is thus over predicted in this region. The advance ratio for the maximum efficiency closely matches the experimental values but the maximum efficiency is estimated at about 10% lower value than the experiments. This is because of the over prediction for power coefficients at high advance ratios. One possible cause may be that the 3d equilibrium condition still depends on the assumption of constant axial induced velocity across the propeller disk. Comparing with JAVAPROP and QPROP, JBLADE gives the best overall results.

Downloaded by UNIV OF TEXAS AUSTIN on August 16, 2013 | http://arc.aiaa.org | DOI: 10.2514/6.2013-4220

Copyright © 2013 by Miguel Angelo Rodrigues Silvestre. Published by the American Institute of Aeronautics and Astronautics, Inc., with permission.

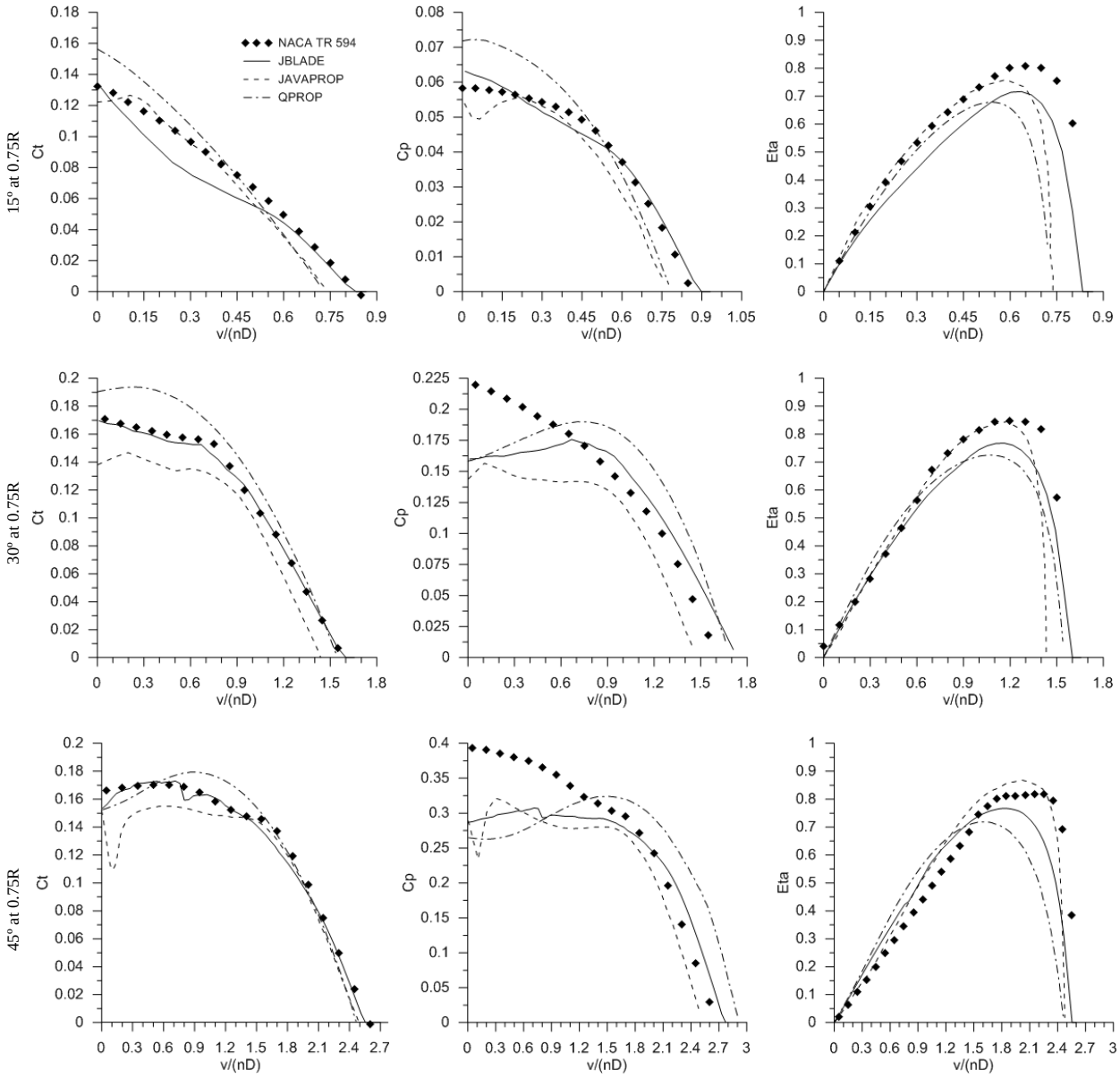

Figure 8. Comparison between data predicted by JBLADE, QPROP[22] and JAVAPROP[27] and data obtained from NACA TR 594[25].

V. Conclusions

JBLADE results prove to be useful for comparison of different propellers designs. Further improvement for the performance prediction at these low advance ratios might be achieved with high fidelity CFD simulations given the suitability of turbulence models to obtain closer to real post stall airfoil characteristics. Nevertheless, CFD is more expensive and JBLADE allows a fast selection of the promising propeller geometry during an optimization procedure.

The modification of the classical BEM for 3D equilibrium provided a significant improvement in the prediction of the propeller performance but more work needs be done on this formulation to reach even better fidelity.

Downloaded by UNIV OF TEXAS AUSTIN on August 16, 2013 | http://arc.aiaa.org | DOI: 10.2514/6.2013-4220

Copyright © 2013 by Miguel Angelo Rodrigues Silvestre. Published by the American Institute of Aeronautics and Astronautics, Inc., with permission.

Acknowledgments

The present work was performed as part of Project MAAT – Multibody Advanced Airship for Transport – with reference no. 285602, supported by European Union through the 7th Framework Programme.

References

[1]Wilson, J. R., "A new era for airships," *Aerospace America*, 2004, pp. 27–31.

[2]Raymer, D. P., Wilson, J., Perkins, H. D., Rizzi, A., Zhang, M., and Puentes, A. R., *Advanced Technology Subsonic Transport Study N + 3 Technologies and Design Concepts - NASA/TM-2011-217130*, Cleveland: 2011.

[3]WANG, X., MA, Y., and SHAN, X., "Modeling of Stratosphere Airship," *Advances in Theoretical and Applied Mechanics*, vol. 2, 2009, pp. 123–142.

[4]Van Eaton, E. H., *Airships and the Modern Military*, Carlisle Barracks: 1991.

[5]Liao, L., and Pasternak, I., "A review of airship structural research and development," *Progress in Aerospace Sciences*, vol. 45, May. 2009, pp. 83–96.

[6]Morgado, J., Silvestre, M. Â. R., and Páscoa, J. C., "Parametric Study of a High Altitude Airship According to the Multi-Body Concept for Advanced Airship Transport - MAAT," *IV Conferência Nacional em Mecânica dos Fluidos, Termodinâmica e Energia*, Lisbon: 2012.

[7]Dumas, A., Trancossi, M., Madonia, M., and Giuliani, I., "Multibody Advanced Airship for Transport," *SAE Technical Paper 2011-01-2786*, 2011.

[8]Ilieva, G., Páscoa, J. C., Dumas, A., and Trancossi, M., "A critical review of propulsion concepts for modern airships," *Central European Journal of Engineering*, vol. 2, Apr. 2012, pp. 189–200.

[9]Rankine, W. M. J., and Froude, R. E., *On the Mechanical Principles of the Action of the Propellers*, Trans Inst Naval Architects (British), 1889.

[10]Drzewiecki, S., *Bulletin de L'Association Maritime*, Paris: 1892.

[11]Betz, A., and Prandtl, L., "Schraubenpropeller mit Geringstem Energieverlust," *Göttinger Nachrichten*, 1919, pp. 193–217.

[12]Eppler, R., and Hepperle, M., "A Procedure for Propeller Design by Inverse Methods," *International Conference on Inverse Design Concepts in Engineering Sciences*, Austin: 1984, pp. 445–460.

[13]Glauert, H., "Airplane propellers," *Aerodynamic theory*, Durand WF, ed., Berlin: 1935.

[14]Goldstein, S., "On the Vortex Theory of Screw Propellers," *Proceedings of the Royal Society A: Mathematical, Physical and Engineering Sciences*, vol. 123, Apr. 1929, pp. 440–465.

[15]Theodorsen, T., *Theory of Propellers*, New York: McGraw-Hill Book Company, 1948.

[16]Larrabee, E. E., "Practical Design of Minimum Induced Loss Propellers," *SAE Technical Paper 790585*, 1979.

[17]Adkins, C. N., and Liebeck, R. H., "Design of optimum propellers," *Journal of Propulsion and Power*, vol. 10, Sep. 1994, pp. 676–682.

[18]Marten, D., Wendler, J., Pechlivanoglou, G., Nayeri, C. N., and Paschereit, C. O., "QBLADE : An Open Source Tool for Design and Simulation of Horizontal and Vertical Axis Wind Turbines," *International Journal of Emerging Technology and Advanced Engineering*, vol. 3, 2013, pp. 264–269.

[19]Marten, D., and Wendler, J., *QBlade Guidelines v0.6*, Berlin: 2013.

[20]Deperrois, A., *Analysis of Foils and Wings Operating at Low Reynolds Numbers - Guidelines for XFLR5 v6.03*, 2011.

[21]Drela, M., "XFOIL - An Analysis and Design System for Low Reynolds Number Airfoils.pdf," *Low Reynolds Number Aerodynamics*, T.J. Mueller, ed., Berlin: Springer-Velag, 1989, pp. 1–12.

[22]Drela, M., *QPROP Formulation*, 2006.

[23]Saravanamuttoo, H., Rogers, G., and Cohen, H., *Gas Turbine Theory*, London: LonSman Group Limited, 1996.

[24]Corrigan, J., and Schillings, J., "Empirical Model for Blade Stall Delay Due to Rotation," *American Helicopter Society Aeromechanics Specialists*, San Francisco: 1994.

[25]Theodorsen, T., Stickle, G. W., and Brevoort, M. J., *Caracteristics of Six Propellers Including the High-Speed Range - Technical Report No. 594*, Langley: 1937.

[26]Morgado, J., Silvestre, M. Â. R., and Páscoa, J. C., "Full Range Airfoil Polars for Propeller Blade Element Momentum Analysis," *Aviation 2013*, Los Angeles: American Institute of Aeronautics and Astronautics, 2013 - accepted for publication.

[27] Hepperle, M., *JavaProp - Design and Analysis of Propellers*, 2010.

Downloaded by UNIV OF TEXAS AUSTIN on August 16, 2013 | http://arc.aiaa.org | DOI: 10.2514/6.2013-4220

Copyright © 2013 by Miguel Angelo Rodrigues Silvestre. Published by the American Institute of Aeronautics and Astronautics, Inc., with permission.